International Journal of Nanomedicine

Dovepress
open access to scientific and medical research

Open Access Full Text Article

ORIGINAL RESEARCH

Recording Electrical Brain Activity with Novel Stretchable Electrodes Based on Supersonic Cluster Beam Implantation Nanotechnology on Conformable Polymers

This article was published in the following Dove Press journal:
International Journal of Nanomedicine

Vadym Gnatkovsky[1]
Alessandro Cattalini[1]
Alessandro Antonini[2]
Laura Spreafico[2]
Matteo Saini[2]
Francesco Noè[1]
Camilla Alessi[1]
Laura Librizzi[1]
Laura Uva[1]
Carlo Efisio Marras[3]
Marco de Curtis[1]
Sandro Ferrari[2]

[1]Unit of Epileptology, Fondazione IRCCS Istituto Neurologico Carlo Besta, Milano, Italy; [2]WISE Srl, Cologno Monzese, Milano, Italy; [3]Neurosurgery Unit, Department of Neuroscience and Neurorehabilitation, IRCCS Bambino Gesù Children's Hospital, Roma, Italy

Background: Multielectrodes are implanted in central and peripheral nervous systems for rehabilitation and diagnostic purposes. The physical resistance of intracranial devices to mechanical stress is critical and fractures or electrode displacement may occur. We describe here a new recording device with stretchable properties based on Supersonic Cluster Beam Implantation (SCBI) technology with high mechanical adaptability to displacement and movement.

Results: The capability of SCBI-based multichannel electrodes to record brain electrical activity was compared to glass/silicon microelectrodes in acute in vitro experiments on the isolated guinea pig brain preparation. Field potentials and power frequency analysis demonstrated equal recording features for SCBI and standard electrodes. Chronic in vivo epidural implantation of the SCBI electrodes confirmed excellent long-term recording properties in comparison to standard EEG metal electrodes. Tissue biocompatibility was demonstrated by neuropathological evaluation of the brain tissue 2 months after the implantation of the devices in the subarachnoid space.

Conclusion: We confirm the biocompatibility of novel SCBI-based stretchable electrode devices and demonstrate their suitability for recording electrical brain activity in pre-clinical settings.

Keywords: brain, field potentials, recording electrodes, supersonic cluster beam implantation

Background

The use of safe and stable implantable medical devices for long-term recording from the nervous system is recognized as one of the challenges of future diagnostic and prosthetic neurology. Multielectrodes chronically implanted in central and peripheral nervous systems have a large impact on cortical and spinal cord stimulation/recording for rehabilitation purposes[1] and for deep brain stimulation in extrapyramidal neurological diseases.[2] In addition, epidural and intracerebral electrodes are routinely utilized for the identification of eloquent areas during brain surgery[3] and are utilized to identify the epileptogenic zone during intracranial explorations in patients candidate to epilepsy surgery.[4,5]

The resistance of the intracranial devices to mechanical stress has been proven to be critical, since long-term qualitative and quantitative alterations of currently used metal intracranial electrodes, such as fractures or electrode displacement, may occur in patients that present with muscular stiffness and dystonic movements.[6] These limitations reveal the need to develop new materials to improve the mechanical resistance of electrodes positioned in close contact to brain tissue for recording/stimulation. Innovative technology and materials have the potential to overcome

Correspondence: Vadym Gnatkovsky
Unit of Epileptology, Fondazione IRCCS Istituto Neurologico Carlo Besta, Via Amadeo, 42, Milano 20133, Italy
Tel +39 0223944518
Email Vadym.Gnatkovsky@istituto-besta.it

submit your manuscript | www.dovepress.com
DovePress
http://doi.org/10.2147/IJN.S224243

limitations in current methods of surface recording. The recent development of a new organic material–based, flexible and scalable neural interface array (NeuroGrid) demonstrated the possibility to record both local field potentials and action potentials from superficial cortical neurons without penetrating the brain surface.[7]

The clinical use of new electrode devices based on novel nanotechnologies and nanomaterials requires preclinical validation, in particular to verify their ability to record electrical brain activity and to test their safety following chronic implantation. The capability to perform these functions long term and without inducing nervous tissue damage are also essential requirements.

We evaluated the ability of a new type of stretchable electrode developed with a novel patented technology, namely the Supersonic Cluster Beam Implantation (SCBI), to record brain tissue electrical activity. SCBI allows metallization of polymers for manufacturing complex microelectronic circuits.[8,9] When stretchable and conformable polymers are used as substrates, the obtained circuits preserve their electrical performances and sustain extensive cycles of stretching and bending.[10] The stretchable property of the connections between recording sites within the array protects against possible ruptures and faults in the recording performance of the device. Preliminary studies demonstrated that cells grow on the metallized layer,[9] indicating that SCBI is biocompatible and suitable for the production of implantable medical devices.

In the present report, the recording performances of SCBI electrode were evaluated in animal models in comparison to brain potentials recorded with standard metal and glass microelectrodes utilized in experimental electrophysiological studies. The brain tissue biocompatibility of SCBI devices was further evaluated after chronic epidural implantation in a preclinical experimental setting. This obligatory validation steps are preliminary to future clinical testing.

Methods

Design and Manufacturing of New SCBI Recording Devices

Highly stretchable and soft recording electrode arrays were developed by means of SCBI technique (WISE – Italian Patent MI2010A000532 - 30/03/2011 and PCT Patent application PCT/EP2011/054903). This technique consists in embedding metal nanoparticles inside a preformed polymer body of the electrode, to form a conductive nanocomposite layer below the surface of the polymer substrate. SCBI is utilized to produce conductive wires, micro-electrodes or complex circuits. More details on the technique are presented elsewhere.[10]

The recording device is sketched in Figure 1A. The recording part of the electrode is made of SCBI implanted platinum (Pt) disk; a gold (Au) connecting line wire is deposited by SCBI technique on a silicone substrate to connect the Pt recording site to the connecting wire; a thin silicone passivation layer is selectively applied on the SCBI gold lines and the interconnector. The fabrication of the device is performed step by step, stacking different layers on a thin silicone substrate. In brief, an Au conducting layer is created by SCBI on the silicone substrate through a stainless steel stencil mask to guide the metal lines. Au is deposited to obtain a resistivity of 1 Ohm/square. This allows the resistance of the metal track to be approximately 10 Ohms. The electrical contacts to the living tissues are then created with Pt SCBI and the terminal points of the Au metal lines by a different stencil mask. Interconnection with wire is made by gluing a Printed Circuit Board (PCB) to the opposite end of the Au lines through a proprietary process described in PCT/IB2017/053056. Finally liquid silicone rubber is selectively dispensed on Au metal lines and the PCB to passivate the conducting layer leaving open the Pt contacts. The process for the electrode manufacturing allows to fabricate arrays of electrodes with size down to 50 μm without using any photolithographic step known to be problematic on soft substrates, to create robust interconnection between rigid wires and soft and stretchable electrodes. While the SCBI deposition technique per se is fully compatible with photolithographic technique and does not have size limitation even down to the micron range, handling highly miniaturized processes on soft substrate is challenging and is not in scope with most of the application currently known for neurorecording and neuromodulation.

For testing purposes arrays with 2–4 recording sites were developed. The shape and size of the electrode are shown in Figure 1B. Each device has two to four Pt recording sites placed at the corners of a 1 x 0.5 mm rectangle. Au lines are connected to a wire through a Printed Circuit Board (PCB). The electric contact was realized by applying sufficient pressures and was stabilized by gluing the two parts together. The wires are then soldered to the PCB.

The mechanical properties of the metal structures deposited on silicones were presented elsewhere.[10] Briefly, the conductive traces maintain their electric properties after more than 50.000 stretching cycles of the polymer up to a strain of 50%. No chemical treatment is required neither before nor after the metallization and the

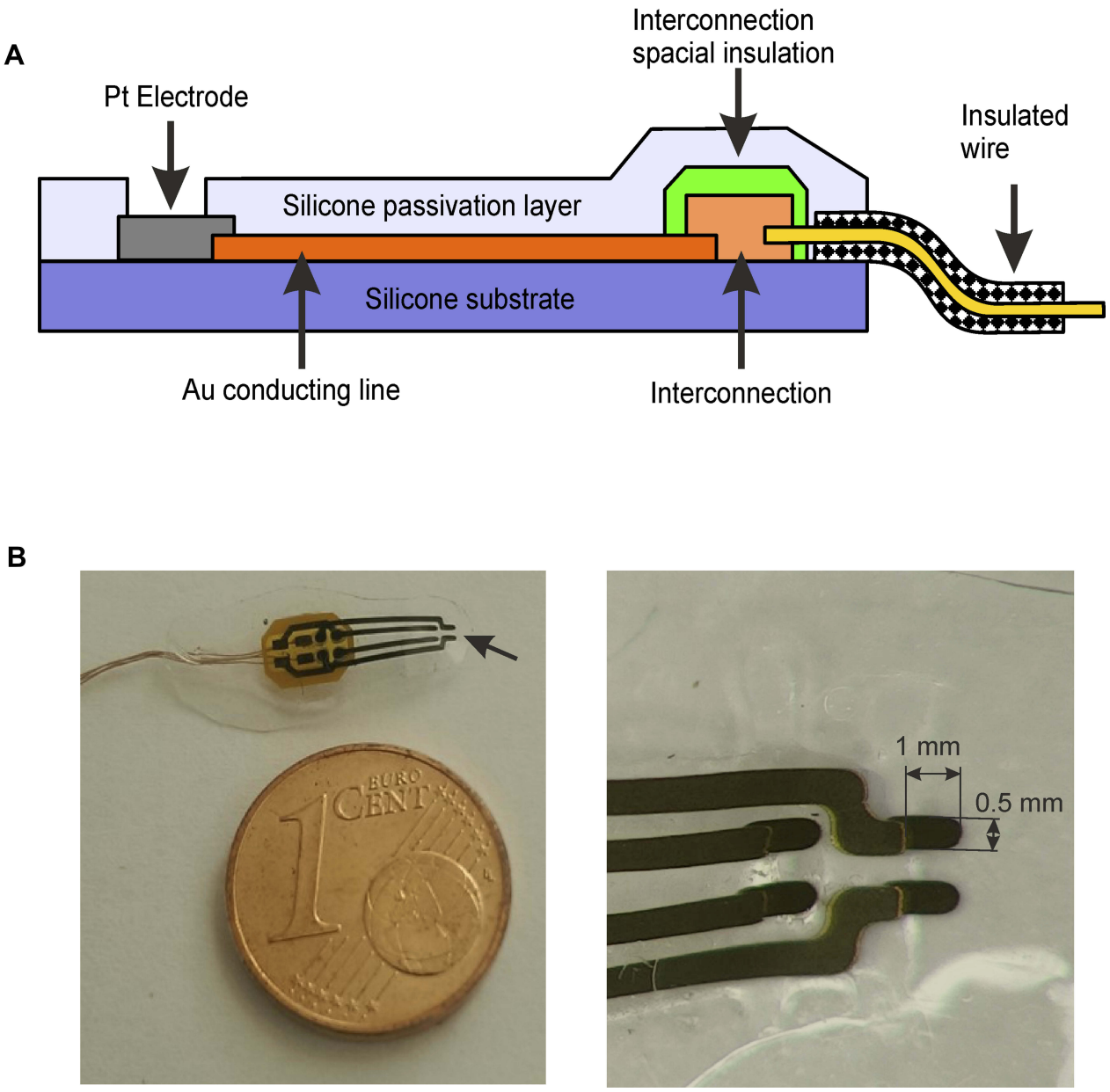

Figure 1 SCBI-based recording device scheme. (**A**) Scheme of the SCBI-based device. The open platinum recording site (grey) and the gold connecting line wire (orange) are deposited on the silicone substrate (purple) with SCBI technique; the silicone passivation cover is illustrated in light purple. (**B**) On the left a four channel electrode. The arrow points at the open end of the 4 Pt recording sites. The overall electrode thickness is 0.2 mm. On the right a close-up picture of the recording leads (1×0.5 mm).

obtained devices are biocompatible, as demonstrated on in cultured neurons.[9]

Preliminary Testing of Recording Devices

The properties of electrodes were tested in a Petri dish filled with physiological-buffered saline solution (PBS) at 25°C, where Electrical Impedance Spectra (EIS) curves taken from 1 to 10^6 Hz and Current-Voltage (CV) curves at 50 mV/s were recorded using an Autolab PGSTAT128 system (Figure 2). Two CV curves were run to equilibrate the electrode behaviour ahead of recording the ones used in the analysis before acquiring the curves for the measurement of the Charge Store Capacity (CSC). The CSC curves were determined between −0.6 V and 0.8 V against an Ag/AgCl reference and a Pt counter electrode. The CSC is the integration of the cathodic part of the resulting curve.

Acute Recording on the in vitro Isolated Guinea Pig Brain

Brains from adult Hartley guinea pigs (N=7, Charles River, Comerio, Italy) weighing 200–250 g were isolated

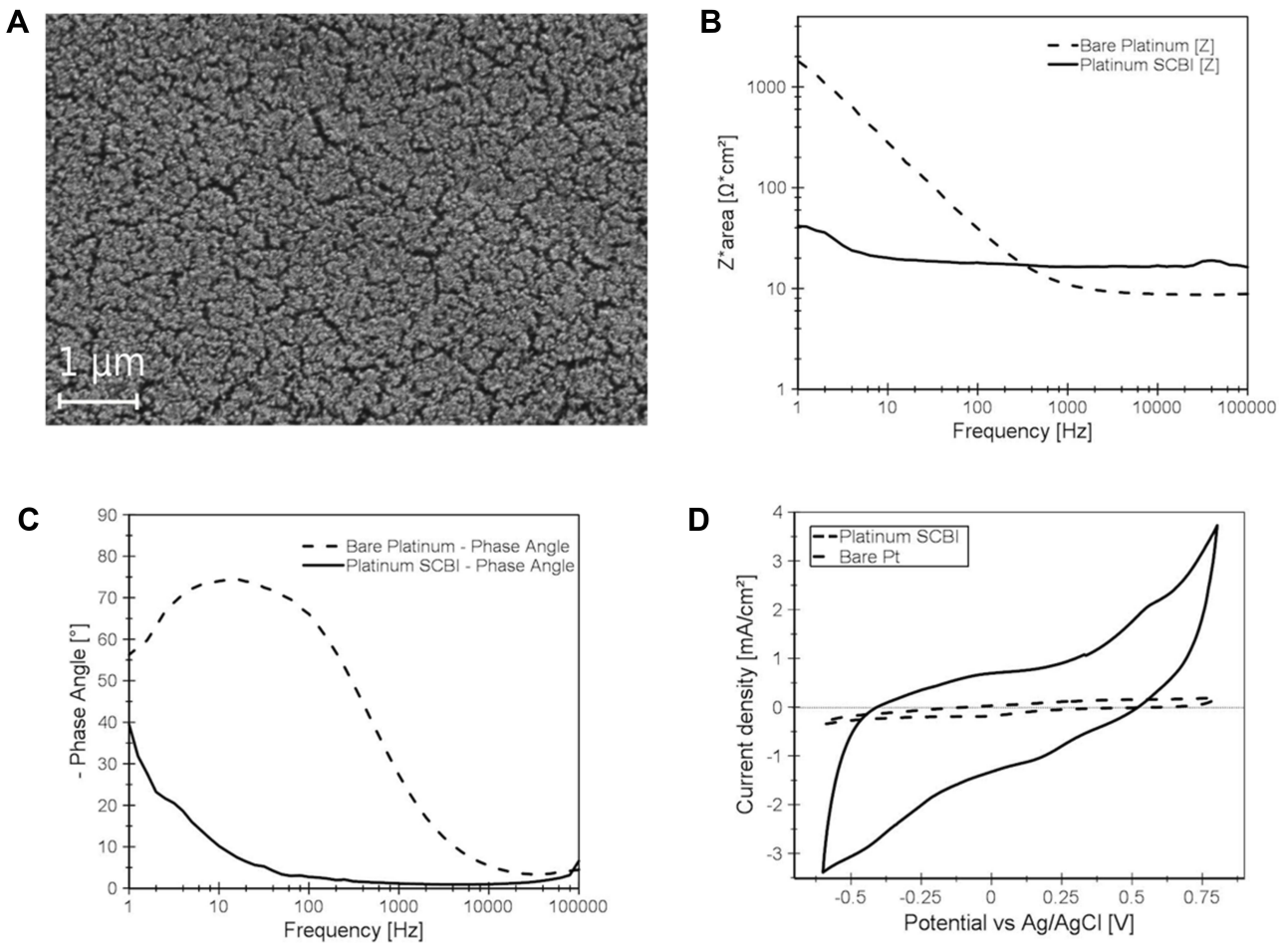

Figure 2 SCBI-based recording device features. (**A**) Scanning electron microscopy (SEM) image of nanostructured platinum electrode surface obtained with SCBI technique. (**B-C**) Electrochemical impedance spectroscopy of 4 mm^2 nanostructured Pt SCBI (continuous lines) and 4 mm^2 bare untreated Pt foil (dashed lines) electrodes. Impedance values (**B**) and angular phase (**C**) are illustrated as a function of the frequency. (**D**) Current-Voltage features of Pt SCBI and Pt foil electrodes measured at 50 mV/s.

in vitro after barbiturate anesthesia (80mg/kg sodium thiopental ip) and were transferred to a perfusion chamber according to the standard protocol.[11,12] A polyethylene cannula inserted in the basilar artery restored brain perfusion with a complex oxygenated saline solution and preserved the isolated brain for up to 6 hrs. The in vitro perfusion of the whole brain was performed at a rate of 6–7 mL/min with a solution composed of NaCl 126 mM, KCl 3mM, KH_2PO_4 1.2 mM, $MgSO_4$ 1.3 mM, $CaCl_2$ 2.4 mM, $NaHCO_3$ 26 mM, glucose 15 mM, 3% dextran MW 70,000 (oxygenated with a 95% O_2-5% CO_2 gas mixture at pH 7.3). Experiments were carried out at 32 °C.

Extracellular recordings were simultaneously performed with the new recording SCBI devices, with a standard glass pipette and with a Michigan silicon probe (iridium contacts; Neuronexus A1x16-5mm-50-177-A16, Ann Arbor, MI, USA; Figure 3). Glass pipettes were forged with a Sutter glass capillary puller (Novato, CA, US) to a final tip size of 10 µm, and were back-filled with 0.9% sodium chloride (3–5 MΩ resistance). Recording contacts of the silicon Michigan electrodes had a size of 15 µm and electrical impedance of 2–3 MΩ. The SCBI-based recording devices had circular shape contacts with diameter = 0.77 mm, exposed recording site area of 0.47 mm^2. Acute extracellular recordings (3 KHz sampling rate, 16bit in DC-mode) were performed for <5 hrs in different areas of the olfactory-limbic cortical region of the in vitro isolated guinea pig brain (see Results). Bipolar twisted silver wire was positioned on the LOT to deliver stimuli (0.1 Hz, 50 µA, 0.1 ms) to evoke responses in olfactory/limbic cortices[13] simultaneously recorded and averaged from the three electrode types, that were amplified via different channels of the same multichannel differential amplifier (Biomedical Engineering, Thornwood, NY, US) and were acquired and analyzed utilizing software (Elpho® - www.elpho.it) developed in Lab VIEW (National Instruments, Austin, TX, USA).

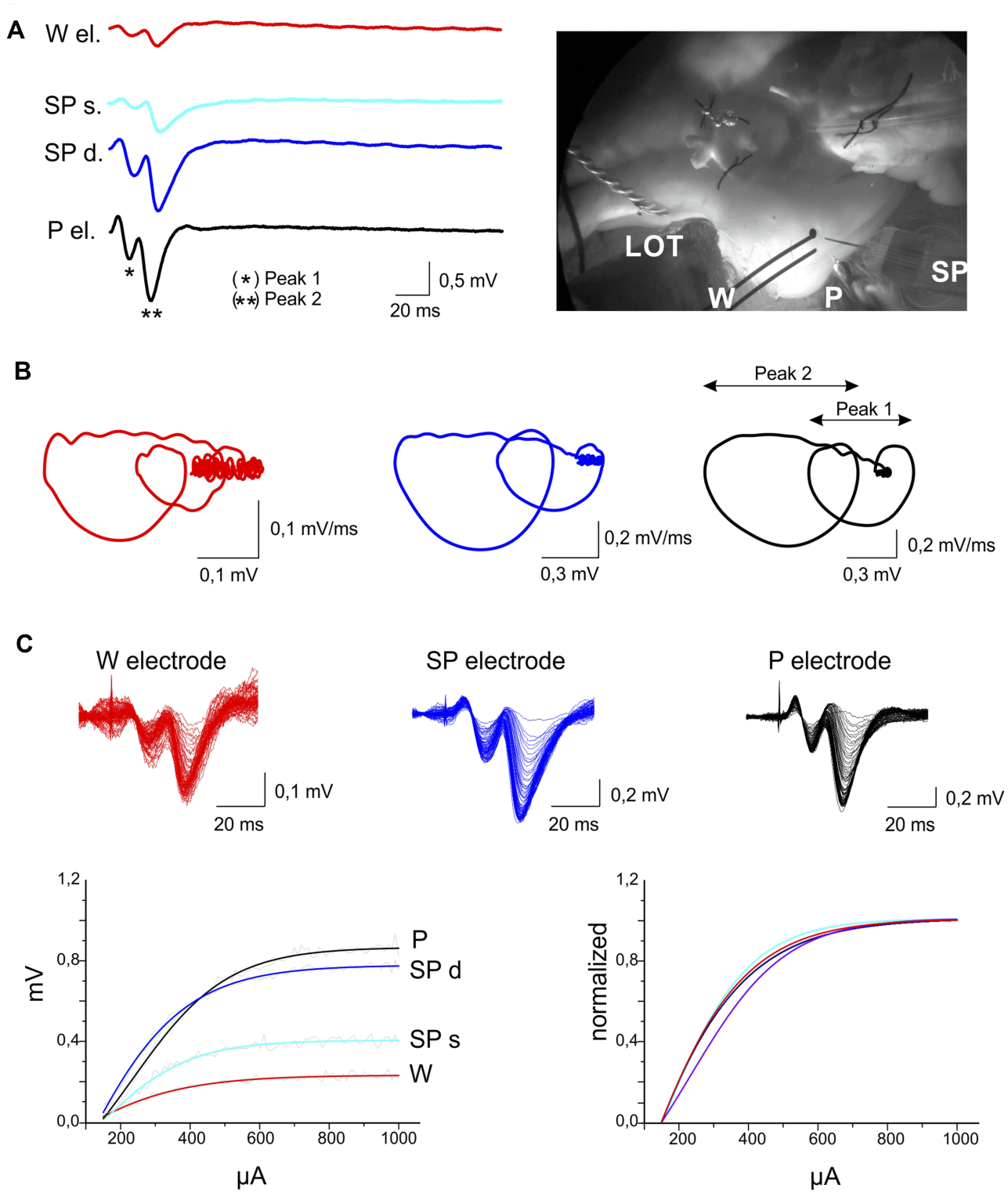

Figure 3 Acute field potential recordings with SCBI-based and standard electrodes. (**A**) Simultaneous electrophysiological recordings performed with SCBI electrodes (W; red traces), a glass micropipette (P; black traces) and a 16-channel silicon probe (SP; blue traces) in the entorhinal cortex of the in vitro isolated guinea pig brain preparation in response to lateral olfactory tract (LOT) stimulation at 0.1 Hz, 50 µA, 0.1 ms (average of five responses); photograph of the electrode setting in the right panel. Two potentials were recorded with the multichannel SP at the pial surface (light blue, SPs) and at 500 µm depth (dark blue; SPd) in the EC. (**B**) Loop trace plots of the averaged evoked responses in the upper rows (peak 1*, peak 2**), performed with W, M and P electrodes. (**C**) The upper part of the panel shows superimposed responses recorded with the three electrode types (color codes as in **A**) during increasing LOT stimulus intensities. Stimulation current was gradually (10 µA steps) increased from 150 to 1000 µA. Averaged CVC (changes in voltage amplitude in response to increasing current stimulation of the LOT) are illustrated in the lower-left panel. Curves normalized for the difference in amplitude due to the depth position of the electrode are illustrated in the right bottom panel.

Chronic Implants and in vivo Recordings

Adult 200–250 g Hartley guinea pigs (N=7, Charles River, Comerio, Italy) housed in a 12 h light-dark environment with ad libitum supply of food and water were anesthetized with 1–4% isoflurane (Abbott Laboratories, Illinois, USA; flow rate 1 lit/min) and were fixed in a stereotaxic frame (SR-6; Narishige, Japan, Tokyo). The skull was exposed and a rectangular cranial window (12x6 mm for the 2-channel electrodes and 12x8 mm for the 4–channel electrodes) was drilled. The window was open on the parietal area of one hemisphere (with the short margin of the cranial window was on the sagittal suture and the posterior along the bregma) to implant two- or four-channel SCBI array devices in the subarachnoid space (Figure 4A). The bone was replaced after positioning the SCBI recording device on the surface of the somatosensory cortex. Two stainless steel screws of 1.1 mm diameter were implanted, EEG electrode on the frontal somatosensory cortex of the contralateral hemisphere and reference electrode into the bone above the cerebellum. The SCBI electrode arrays have rectangular shape contacts 1 × 0.5 mm, exposed recording site area of 0.5 mm^2, while the screws have an exposed area of approximately 0.7 mm^2. All electrodes were fixed on the skull by acrylic cement (Paladur, Heraeus, South Bend, US). After surgery, animals were treated with subcutaneous injections of both 1.1 mg/kg flunixin (Finadyne; Schering Ploug, Kenilworth, NJ, US; every 12 h for 5 days) and 2.5% enrofloxacin (Baytril; Bayer, Leverkusen, Germany, for 7 days).

One week and 1 month after surgery, EEG monitoring with a BrainQuick System by Micromed (Mogliano Veneto, Italy) was performed 24/24 hrs for 3 consecutive days. The implanted electrodes were connected to the recording amplifier through a pedestal connector (Plastic One, Roanoke, US) and EEG data were recorded wide-band, 0.1–2.0 kHz, and were sampled at 2 kHz/channel with 12-bit precision (System Plus Evolution; Micromed, Mogliano Veneto, Italy).

Histological Controls

Two months after electrode implantation, animals were anesthetized with sodium thiopental (125 mg/kg i.p., Farmotal; Pharmacia, Milano, Italy) and were transcardially perfused with 1% sodium sulfide in 0.1 M phosphate buffer for 4 min, followed by 1% glutaraldehyde and 4% paraformaldehyde in phosphate buffer (0.1 M) for 5 min. After brain fixation, the skull was opened and the epidural recording devices were carefully removed. Guinea pig brains were explanted and were immersed in 4% paraformaldehyde before cutting 50 µm coronal sections processed for thionine 0.1% (standard protocol) and immunohistochemical staining. For immunohistochemistry, sections were washed for 10 min in 3% hydrogen peroxide in phosphate buffer to inactivate endogenous peroxidase. After blocking nonspecific sites in

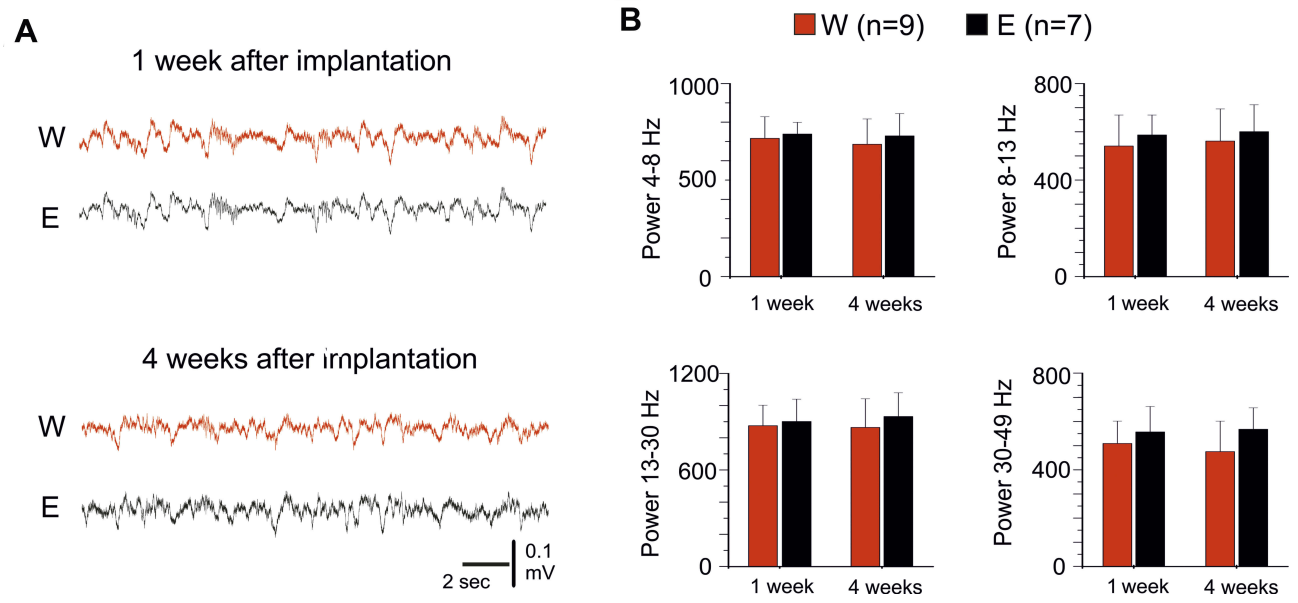

Figure 4 Chronic recordings with implanted epidural SCBI electrodes. (**A**) Sample recordings performed with E and W electrodes in the same guinea pig, 1 week and 1 month after the electrode implant. (**B**) Averaged frequency power densities of EEG signals recorded with standard E electrodes (black columns) and with SCBI probes (red columns), 1 week and 1 month after surgical electrode implant. Different frequency bands were separately analyzed (4–8 Hz, 8–13 Hz, 13–30 Hz and 30–50 Hz) in 9 W and 7 E (control) electrodes.

phosphate buffer (10% normal goat serum and 0.2% Triton-X 100), sections were incubated overnight at 4°C with polyclonal antibody anti glial fibrillary acid protein (1% normal goat serum; anti-GFAP 1:1,000; Sigma, Milano, Italy). After rinsing in phosphate buffer solution, sections were incubated for 75 min in biotinylated goat anti-rabbit immunoglobulin (Vector Laboratories, Burlingame, CA, USA) diluted 1:200 in 1% normal goat serum in phosphate buffer. The avidin-biotin-peroxidase protocol (ABC; Vector Laboratories) was followed and 3,3-diaminobenzidine tetrahydrochloride (Sigma) was used as chromogen. Finally, sections were mounted, dehydrated, and cover-slipped with distyrene plasticizer xylene. Thionine and immunostaining with GFAP-antibodies were utilized to monitor brain damage in proximity of the SCBI recording electrode device. Coronal sections were visualized using the Scanscope software (Aperio Technologies, CA, US). Thionine and GFAP staining were analyzed by quantitative field fraction estimates carried out using Image-Pro Plus 7 software (Media Cybernetics, Inc. MD, US). The percentage of specific staining density was estimated in 2 mm^2 rectangular regions of interest (ROIs; Figure 5A) positioned on the somatosensory cortex. Neuronal and GFAP density in each ROI were automatically calculated by the software in each hemisphere on two adjacent slices per animals.

The experimental protocols were reviewed and approved by the Committee on Animal Care and Use and by the Ethics Committee of the Fondazione Istituto Neurologico, in accordance with the European Committee Council Directive (86/89/EEC). Efforts were made to minimize the number of animals used and their suffering.

Statistical analysis was performed using OriginPro 2016. Data are expressed as mean ± standard deviation. Statistical analysis was performed utilizing ANOVA One Way after verifying the data distribution with the Kolmogorov-Smirnov normality test. The difference between mean measurements was considered statistically significant with Tukey's test for p values lower than 5% (0.05).

Results and Discussion

We first analysed the general properties of SCBI electrodes. Figure 2A shows the surface of the SCBI deposited the Pt surface nanostructure at high magnification. The roughness of the nanostructure surface is the result of the agglomeration taking place during the SCBI process. The nanoparticles sprayed by the nanocluster source coalesce at the silicone surface, forming a nanometre fractal structure that results in a metal surface with a very large specific surface area. The Pt electrodes properties were studied by impedance spectroscopy and current-voltage response features. To characterize the intrinsic properties of the nano-rough metal analyses were performed on 4 mm^2 Pt electrodes were considered during electrochemical analysis. Figure 2B shows the comparison between 4 mm^2 SCBI based electrode (continuous line) and an electrode having the same geometric area, but made of a plain platinum foil (dashed lines). SCBI Pt electrodes consistently show impedance at 1 Hz close to 30 Ω/cm^2 while Pt foil has an impedance of roughly 2000 Ω/cm^2. The phase of the impedance as a function of the frequency revealed an extended resistive behaviour of the SCBI electrode, as compared to the Pt foil (Figure 2C).[14,15] Impedance at low frequency for Pt electrodes provides an indication of the real surface area for a given geometric electrode area. A low impedance at 1 Hz indicates a large specific surface area that provides high charge storage capacity, low polarization in the presence of slowly fluctuating potentials thus improving the quality of long-term recording and a better signal-to-noise ratio.[16] Figure 2D shows a comparison of the Current-Voltage Curves (CVC) of SCBI based electrodes against the standard Pt foil electrode. The large capacitive component presented by the SCBI based electrode can be entirely attributed to the difference in specific surface area. We calculated the cathodal CSC from the time integral of the cathodic current in a slow-sweep-rate cyclic voltammogram over a potential range within the water electrolysis window.[17] The calculated CSC for the SCBI platinum electrode was 38 mC/cm^2, as opposed to the platinum foil that showed a CSC of 0.55 mC/cm^2 (Figure 2D). This leads to a 70x difference in specific surface area between the two materials, as shown in the literature for nanostructured Pt surfaces in coated electrodes; remarkably we obtained high electrode performances natively, rather than through a post-deposition or post-processing method and in the case of coated electrodes.[18] These data demonstrate that SCBI-based electrode surface has ideal properties for electric activity recording.

Acute Electrophysiological Testing

Recording properties of the new devices were first tested in the in vitro isolated guinea pig brain. Field potentials recorded with SCBI-based probes and with glass micropipette and multichannel silicon electrodes were compared. As illustrated in the representative experiment of Figure 3, responses evoked by electrical stimulation of the LOT were simultaneously recorded in the entorhinal cortex (EC) with a SCBI-based stretchable electrode (*W*; red traces), a silicon-structured probe (*SP*; blue traces) and

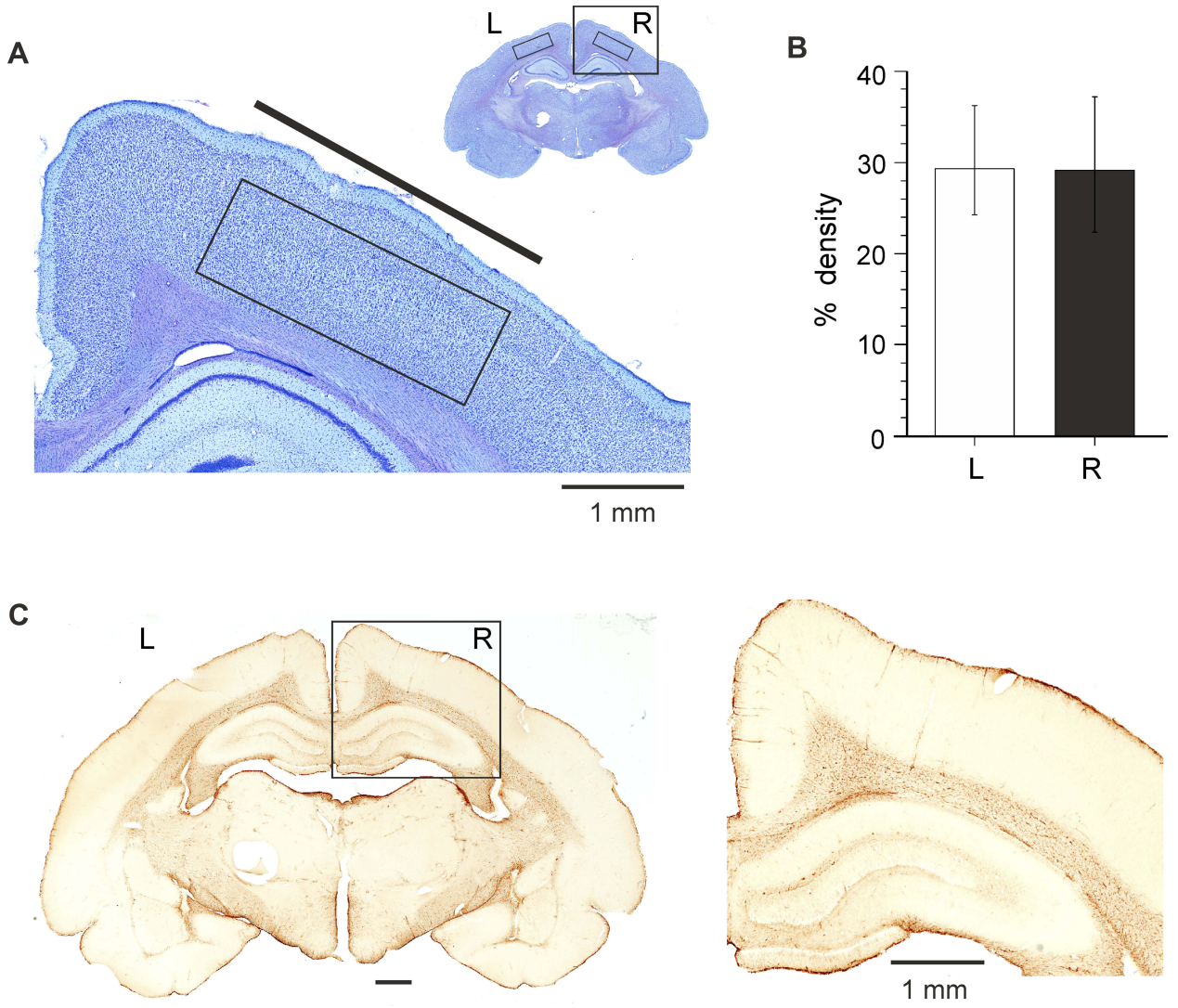

Figure 5 Neuropathological analysis of brain tissue 2 months after implantation of SCBI electrodes in the epidural space over the fronto-parietal cortex of the left hemisphere. (**A**) Thionine-stained sample coronal section of an electrode-implanted guinea pig brain. The boxes outline the areas utilized to perform quantitative densitometric measurements. The cortical area included in the box of the inset is illustrated at higher magnification. (**B**) Average data obtained by densitometric measurements (% staining density) performed on the right and left frontoparietal cortical areas (two slices per animal) in six guinea pigs chronically implanted with SCBI electrodes. (**C**) GFAP-stained section of a coronal section of the brain of a guinea pig implanted with SCBI electrode over the left frontoparietal cortex (and a metal epidural electrode on the right hemisphere); the boxed area is magnified on the right.

a glass recording pipette (*P*; black traces); signals were acquired with the same recording amplifier, referenced to a common Ag/AgCl electrode placed in the recording chamber. The *W* electrode was placed on the EC surface. The distance between recording sites was 0.8–0.9 mm. The amplitude of the evoked response (average of five responses) recorded with *W* was similar to that recorded with the superficial *SP* lead (*SPs*) positioned in the EC pial surface (first peak 0.14 vs 0.12 mV, second peak 0.31 vs 0.48 mV, Figure 3A). *P* and *SPd*, both positioned at 500 µm depth in the EC, recorded larger amplitude potentials (first peak 0.55 and 0.64 mV, second peak 1.08 and 1.28 mV correspondingly) compared to *W* and *SPs*, as expected from a depth electrode inserted into the cortical tissue. The difference in amplitude was due to the electrode depth position and not to the recording performances of the SCBI electrode. To compare dynamic changes of the evoked field potentials, the first derivate of the recorded signals (dV/d*t* measured as mV/ms; *y*-axis) was plotted against the instantaneous signal amplitude (measured as mV; *x*-axes); averaged field potentials are represented as loop traces, in which the starting point represents the onset potential, and the extreme left peak is the maximal voltage amplitude (peak 1 – small loop, peak 2 – big loop); the upper and lower parts of the loop describe the depolarization and repolarization kinetics, respectively (Figure 3B).

Voltage responses evoked by increasing LOT stimulation amplitudes (CVC) were recorded with *W, P* and *SPp* (red, blue and black in the upper superimposed traces of Figure 3C) and show similar dynamics in all three electrode types, as also demonstrated by the CVC in the lower panels of Figure 3C (normalized for the difference in signal amplitude in the right panel).

In summary, brain surface recording performances of SCBI electrodes were comparable to both surface and intra-cortical signals recorded by both glass pipettes and silicon-probes.

Chronic Electrophysiology and Neuropathology Testing in vivo

Electrocorticographic recordings were simultaneously performed in seven guinea pigs with a standard epidural metal screw electrode (E) positioned on the right hemisphere and a SCBI-based electrode (*W*) implanted between the dura and the skull in the epidural space above the frontoparietal cortex of the left hemisphere (Figure 4). In three animals, recordings were performed with 2-channel SCBI electrodes. One and four weeks after the surgical implant, signals were continuously recorded for 3 days (sample traces in Figure 4A, Supplementary Video 1 and 2). Averaged power spectrum analysis of 10 twenty-second epochs performed 1 week after surgery demonstrated that all investigated EEG frequency components were similarly expressed in power density a recorded with *E* (Figure 4B; Controls; n=7) and *W* electrodes (n= 9 recording sites in six guinea pigs); 1 month after implantation the preservation of the EEG signal power in all explored EEG frequencies (theta at 4-8Hz; alpha at 8–13 Hz; beta at 13–30 Hz and gamma at 30–50 Hz) for both electrode types was confirmed. Reduced EEG amplitude was observed in one guinea pig in which a subdural hematoma was found at neuropathological examination (see below).

Biocompatibility of the presented SCBI based electrodes has been assessed through the standard ISO10993-1 approach (data not presented). Cytotoxicity, sensitization, irritation, acute systemic toxicity, pyro- and geno-toxicity were demonstrated. Since standard biocompatibility tests use device extracts to assess biological effects, the local effects arising from direct contact of the device to the biological tissues can only be studied by long term follow-up on animal implants.

Two months after the electrode implant, the animals were sacrificed and the brains were extracted and fixed in 4% paraformaldehyde after removing the epidural electrodes. In one guinea pig, clear signs of cortical hemorrhage were observed in the right frontoparietal region, likely due to the implant procedure; in this animal the recording from this SCBI electrode was marred by artifacts. This animal was excluded by subsequent analysis. Densitometric thionine staining measurements (n=6 guinea pigs, Supplementary Table 1) performed on 2 mm^2 areas in two 50 µm coronal sections per animal demonstrated no difference between the cell staining in cortical regions under the implanted SCBI-based electrode and the contralateral homologous cortex (29.850 ± 6.610% and 29.244 ± 7.545% in left and right hemispheres, respectively; p 0.703 at Tukey's test; Figure 5B). The quantification of GFAP immunostaining (Figure 5C) showed no significant difference (p=0.074; n=6) between the neocortex under the epidural SCBI electrode (0.005 ± 0.006%) compared to the contralateral homologous region (0.019 ± 0.025%). The data demonstrate that the cortical tissue under after the SCBI electrode is not altered 2 months after the implantation.

We demonstrate here the recording proficiency and the biocompatibility of a new, stretchable type of probe build on SCBI nanotechnology. The new electrodes have low impedance and large surface, ideal suited to record field activities from brain tissue, as demonstrated in acute in vitro experiments, where the SCBI electrode performances are compared against the laboratory controlled optimal recording conditions performed by standard electrodes. Our results demonstrate that electrodes based on SCBI nanotechnology can reliably sample the evoked neuronal activity with kinetics that are similar to the reference signal recorded with standard research high-quality probes. The difference in amplitude observed in comparison to metal electrodes is due to the smaller resistance of the stretchable probes (larger recording surface) and does not affect signal dynamics, since similar CVC were recorded with both types of electrodes. The granular nanoscale surface of the SCBI conductive electrode greatly improves the area of contact with tissue. This unique characteristic opens an important perspective for direct current recording (DC) and for better current distribution during stimulation protocols performed with SCBI probes.[19–21]

New technologies for multimodal neural implants have been developed to advance diagnostic neurophysiological recording.[22–25] However, the long-term biocompatibility and mechanical incongruity between soft neural tissues and hard implants remain an important concern for therapeutic application.[26–28] Neural implant based on flexible transparent silicone substrate with stretchable gold interconnects was successfully used to restore locomotion after spinal cord injury in freely behaving animals.[29] Novel, non-penetrating

surface array (NeuroGrid) composed of "soft" organic electronics, demonstrates the possibility to record action potentials from superficial cortical layers of rodents and humans within the extended duration.[7] The features of the devices described in the present report were developed to record local field potential activity from the pial surface, for a potential future clinical use in alternative to the grid-strip electrodes currently available. The flexible silicone base of our electrodes demonstrates ideal properties to effectively adhere brain surface without significant damage of the underlying tissue; the stretchable conductive part of the electrode is strong enough to resist long-term mechanical stress possibly occurring during chronic in vivo recordings. Moreover, the possibility to produce variable form, size and the number/density of recording contacts by SCBI technique is essential for intracranial multi-electrode arrays that record from the surface of the human brain (grid and strip electrodes). This is a prerequisite to record EEG signals with high spatial and temporal resolution from the surface of the cortical circumvolutions. While flexibility of the supporting material will adapt the surface of the recording sites to the curvature of cortex, recording from deep structures of the human brain is still a critical issue.

Finally, we expect good signals and less sensitivity to motion at stretchable points such as the connections between the probe and the cables and between the single recording sites of the electrode array, in comparison to rigid and less flexible conventional electrodes. Less mechanical disturbance during chronic or intra-operative recordings from spinal nerve roots or peripheral nerves can be achieved with flexible materials in comparison to more rigid electrodes presently in commercial use.[30–32] Flexible and stretchable electrode material will also be more resistant to hypermotor and dystonic events.

Conclusion

The study demonstrates electrochemical stability, mechanical robustness and long-term functionality of the SCBI-based stretchable electrodes, fulfilling the challenging requirements for long-term implantation.

Consent for Publication

All authors consent the publication of the data included in the present report.

Abbreviations

EEG, Electroencephalography; CSC, Charge Store Capacity; CVC, Current-Voltage Curves; EIS, Electrical Impedance Spectra; EC, Entorhinal Cortex; GFAP, Glial Fibrillary Acid Protein; LOT, Lateral Olfactory Tract; PCB, Printed Circuit Board; SCBI, Supersonic Cluster Beam Implantation.

Ethical Publication Statement

We confirm that we have read the Journal's position on issues involved in ethical publication and affirm that this report is consistent with those guidelines.

Ethics Approval

The experimental protocols were reviewed and approved by the Committee on Animal Care and Use and by the Ethics Committee of the Fondazione Istituto Neurologico.

Availability of Data and Material

Data and materials are available upon request.

Funding

The study is supported by the Italian Health Ministry grant RF-2010-2304417.

Disclosure

WISE Srl is a Medical Device Company involved in electrodes development for neuromonitoring and neuromodulation. Alessandro Antonini, Laura Spreafico, Matteo Saini, and Sandro Ferrari are employees in WISE Srl. Dr Sandro Ferrari reports a patent PCT/EP2011/054903 issued. The authors report no other conflicts of interest in this work.

References

1. Borton D, Micera S, Millan JDR, Courtine G. Personalized neuroprosthetics. *Sci Transl Med*. 2013;5(210):210.
2. Cif L, Vasques X, Gonzalez V, et al. Long-term follow-up of DYT1 dystonia patients treated by deep brain stimulation: an open-label study. *Mov Disord*. 2010;25(3):289–299. doi:10.1002/mds.22802
3. MacDonald DB, Dong C, Quatrale R, et al. Recommendations of the International Society of Intraoperative Neurophysiology for intraoperative somatosensory evoked potentials. *Clin Neurophysiol*. 2019;130(1):161–179. doi:10.1016/j.clinph.2018.10.008
4. Cardinale F, Cossu M, Castana L, et al. Stereoelectroencephalography: surgical methodology, safety, and stereotactic application accuracy in 500 procedures. *Neurosurgery*. 2013;72(3):353–366.
5. Gonzalez-Martinez J, Bulacio J, Alexopoulos A, Jehi L, Bingaman W, Najm I. Stereoelectroencephalography in the "difficult to localize" refractory focal epilepsy: early experience from a North American epilepsy center. *Epilepsia*. 2013;54(2):323–330.
6. Marras C, Rizzi M, Ravagnan L, et al. Morphological and chemical analysis of a deep brain stimulation electrode explanted from a dystonic patient. *J Neural Transm*. 2013;120(10):1425–1431.
7. Khodagholy D, Gelinas JN, Thesen T, et al. NeuroGrid: recording action potentials from the surface of the brain. *Nat Neurosci*. 2015;18(2):310–315.

8. Ravagnan L, Divitini G, Rebasti S, Marelli M, Piseri P, Milani P. Poly(methyl methacrylate)–palladium clusters nanocomposite formation by supersonic cluster beam deposition: a method for microstructured metallization of polymer surfaces. *J Phys D Appl Phys*. 2009;42(8):082002.
9. Marelli M, Divitini G, Collini C, et al. Flexible and biocompatible microelectrode arrays fabricated by supersonic cluster beam deposition on SU-8. *J Micromech Microeng*. 2011;21(4):045013.
10. Corbelli G, Ghisleri C, Marelli M, et al. Highly deformable nanostructured elastomeric electrodes with improving conductivity upon cyclical stretching. *Adv Mater*. 2011;23:4504–4508. doi:10.1002/adma.201102463
11. de Curtis M, Pare D, Llinas RR. The electrophysiology of the olfactory-hippocampal circuit in the isolated and perfused adult mammalian brain in vitro. *Hippocampus*. 1991;1(4):341–354.
12. de Curtis M, Biella G, Buccellati C, Folco G. Simultaneous investigation of the neuronal and vascular compartments in the guinea pig brain isolated in vitro. *Brain Res Protoc*. 1998;3(2):221–228. doi:10.1016/S1385-299X(98)00044-0
13. Biella G, de Curtis M. Associative synaptic potentials in the piriform cortex of the isolated guinea-pig brain in vitro. *Eur J Neurosci*. 1995;7(1):54–64. doi:10.1111/ejn.1995.7.issue-1
14. Desai SA, Rolston JD, Guo L, Potter SM. Improving impedance of implantable microwire multi-electrode arrays by ultrasonic electroplating of durable platinum black. *Front Neuroeng*. 2010;3:5.
15. Boretius T, Jurzinsky T, Koehler C, Kerzenmacher S, Hillebrecht H, Stieglitz T. High-porous platinum electrodes for functional electrical stimulation. 2011 Annual International Conference of the IEEE Engineering in Medicine and Biology Society; IEEE; 2011:5404–5407. Boston, MA, USA.
16. Harris AR, Allitt BJ, Paolini AG. Predicting neural recording performance of implantable electrodes. *Analyst*. 2019;144(9):2973–2983. doi:10.1039/C8AN02214C
17. Cogan SF. Neural stimulation and recording electrodes. *Annu Rev Biomed Eng*. 2008;10(1):275–309. doi:10.1146/annurev.bioeng.10.061807.160518
18. Boehler C, Stieglitz T, Asplund M. Nanostructured platinum grass enables superior impedance reduction for neural microelectrodes. *Biomaterials*. 2015;67:346–353.
19. Vanhatalo S, Voipio J, Kaila K. Full-band EEG (FbEEG): an emerging standard in electroencephalography. *Clin Neurophysiol*. 2005;116(1):1–8. doi:10.1016/j.clinph.2004.09.015
20. Ikeda A, Taki W, Kunieda T, et al. Focal ictal direct current shifts in human epilepsy as studied by subdural and scalp recording. *Brain*. 1999;122(5):827–838.
21. Kuck A, Stegeman DF, van Asseldonk EHF. Modeling trans-spinal direct current stimulation in the presence of spinal implants. *IEEE Trans Neural Syst Rehabil Eng*. 2019;27:790–797.
22. Kim D-H, Viventi J, Amsden JJ, et al. Dissolvable films of silk fibroin for ultrathin conformal bio-integrated electronics. *Nat Mater*. 2010;9(6):511–517. doi:10.1038/nmat2745
23. Fattahi P, Yang G, Kim G, Abidian MRA. Review of organic and inorganic biomaterials for neural interfaces. *Adv Mater*. 2014;26(12):1846–1885.
24. van den Brand R, Heutschi J, Barraud Q, et al. Restoring voluntary control of locomotion after paralyzing spinal cord injury. *Science*. 2012;336(6085):1182–1185. doi:10.1126/science.1217416
25. Park D-W, Schendel AA, Mikael S, et al. Graphene-based carbon-layered electrode array technology for neural imaging and optogenetic applications. *Nat Commun*. 2014;5(1):5258. doi:10.1038/ncomms6258
26. Barrese JC, Rao N, Paroo K, et al. Failure mode analysis of silicon-based intracortical microelectrode arrays in non-human primates. *J Neural Eng*. 2013;10(6):066014. doi:10.1088/1741-2560/10/6/066014
27. Moshayedi P, Ng G, Kwok JCF, et al. The relationship between glial cell mechanosensitivity and foreign body reactions in the central nervous system. *Biomaterials*. 2014;35(13):3919–3925. doi:10.1016/j.biomaterials.2014.01.038
28. Potter KA, Jorfi M, Householder KT, Foster EJ, Weder C, Capadona JR. Curcumin-releasing mechanically adaptive intracortical implants improve the proximal neuronal density and blood–brain barrier stability. *Acta Biomater*. 2014;10(5):2209–2222. doi:10.1016/j.actbio.2014.01.018
29. Minev IR, Musienko P, Hirsch A, et al. Electronic dura mater for long-term multimodal neural interfaces. *Science*. 2015;347(6218):159–163. doi:10.1126/science.1260318
30. Lee WS, Lee JK, Lee SA, Kang JK, Ko TS. Complications and results of subdural grid electrode implantation in epilepsy surgery. *Surg Neurol*. 2000;54(5):346–351.
31. Onal C, Otsubo H, Araki T, et al. Complications of invasive subdural grid monitoring in children with epilepsy. *J Neurosurg*. 2003;98(5):1017–1026.
32. Simon SL, Telfeian A, Duhaime A-C. Complications of invasive monitoring used in intractable pediatric epilepsy. *Pediatr Neurosurg*. 2003;38(1):47–52.